ADVANCED FUNCTIONAL MATERIALS
www.afm-journal.de

Nano/Micromotor-Driven SERS for Highly Sensitive and Spatially Controlled Sensing

I. Brian Becerril-Castro, Veronica Salgueiriño, Miguel A. Correa-Duarte,* and Ramon A. Alvarez-Puebla**

Nano/micromotors (NMs) are tiny structures capable of converting various forms of energy into mechanical motion at the micro and nanoscale. These motors operate in environments characterized by low inertia and low Reynolds numbers. The potential applications of NMs are vast, particularly in the fields of biomedicine and environmental science. One of the most intriguing developments in this field is the integration of NMs with surface-enhanced Raman scattering (SERS) spectroscopy. SERS is a powerful analytical technique that enhances the Raman intensity of molecules, allowing for highly sensitive detection and analysis of trace amounts of substances. This integration offers highly precise and localized ultrasensing capabilities. The combination of NMs with SERS can also facilitate real-time imaging inside living organisms. This has immense potential in chemical and cell biology and medical diagnostics and prognosis. Herein this review describes the types of NMs and their fabrication, the incorporation of plasmonic nanostructures, capable of creating strong electromagnetic fields when illuminated by light, which in turn enhances the Raman signals significantly, their applications, and their future prospects in areas such as precision medicine, environmental monitoring, and possibly even in new realms like microscale robotics and targeted therapeutics.

1. Introduction

Nano/micromotors (NMs) are structures capable of transforming different kinds of energy into mechanical movement at the micro and nanoscale, that is, in regimes with no inertia and low Reynolds number.[1] Because of their small size, NMs hold dreamy goals such as working as small machines entering the organism to perform surgeries from the interior or even assisting defective organs.[2] Regardless, they are a well-known and active field, which have shown potential in biomedical and environmental applications such as sensing,[3] imaging,[4] cargo delivery,[5] microscale manipulation,[6] biological media exploration,[7] as well as environmental cleaning and monitoring.[8] These former advances in applications that rely on the nano/micro scale movement of NMs position them as attractive candidates for their integration with surface-enhanced Raman scattering (SERS) spectroscopy. SERS spectroscopy is an analytical technique that provides comprehensive chemical and structural information of analytes, thus allowing their detection and identification down to the single molecule level.[9] SERS relies on the enhancement of the typically low Raman scattering intensity of molecules, mainly by an increase in the local electric field at the molecule through the use of plasmonic surfaces.[10] Upon illumination, the Raman intensity is increased in factors that can reach over 10^{10}.[11]

The integration of SERS with NMs seeks to join the capacity to signalize the presence of analytes of the SERS technique with the controlled movement of NMs to obtain a highly sensitive and spatially controlled sensing technique. This association can improve the capabilities of NMs in multiple scenarios. For example, increasing the sensibility and specificity of NMs-based sensing applications. Moreover, SERS active NMs could be efficiently directed to the interest zone for the detection of multiple compounds (including inorganic molecules and ions[12] as well as biological analytes[13]) and imaging in vivo applications inside cells.[14] This intracellular monitor possibility is compelling because of the multiple examples of self-guided NMs toward and inside cells that have been reported.[15] Alternatively, SERS active NMs provide an effective option to retrieve information from the surrounding media. The

I. B. Becerril-Castro, R. A. Alvarez-Puebla
Department of Physical and Inorganic Chemistry
Universitat Rovira i Virgili
Tarragona 43007, Spain
E-mail: ramon.alvarez@urv.cat
V. Salgueiriño, M. A. Correa-Duarte
CINBIO
Universidade de Vigo
Vigo 36310, Spain
E-mail: vsalgue@uvigo.es; macorrea@uvigo.es
R. A. Alvarez-Puebla
ICREA—Institució Catalana de Recerca i Estudis Avançats
Barcelona 08010, Spain

The ORCID identification number(s) for the author(s) of this article can be found under https://doi.org/10.1002/adfm.202314084

DOI: 10.1002/adfm.202314084

common use of fluorescent markers on imaging applications with NMs could be improved for multiplex imaging using SERS-encoded nanoparticles (NPs) while reducing the possibility of photobleaching. An interesting new characteristic of the incorporation of SERS spectroscopy with NMs, is the molecular enrichment on the sensing surface due to the mechanical movement of the NMs. This enrichment increases the limit of detection of SERS active NMs compared with their static counterparts.

The synergy between NMs and SERS has just begun to be explored. In this review we intend to discuss the main approaches to endorse NMs with SERS capabilities for the improvement of existing applications, signaling potential new applications, and providing possible directions in this promising field.

2. Nano/Micromotors

Nanomotor's main feature is the capacity to perform controlled movement and achieve tasks at the micro and nanoscale. They can be classified either as a function of their morphology or by the source of energy. Among the different morphologies found in NMs, Janus particles,[16] metallic wires, tubular structures,[17] and helical shapes[18] are among the most popular. Although more complex or different NMs morphologies exist in the literature such as bowls,[19] matchstick-shaped,[20] bullet-shape,[21] or brush-like,[22] they tend to follow the same principle: break the symmetry to produce translational movement. This pattern appears because the movement of NMs occurs at low Reynolds numbers (down to $\approx 10^{-5}$)[23] and against the Brownian motion.[24] On one side the Brownian motion establishes a minimum threshold for the necessary force to achieve movement while the low Reynolds number means that approaches to movement that rely on inertial forces or the use of symmetrical movements are no longer possible. Thus, the NMs need to break the symmetry in order to create a local thrust gradient on the NMs that results in net movement.[25] To do so, NMs can use asymmetric movements,[26] have non-symmetrical surface chemical or physical reactions,[27] possess asymmetric compositions or morphologies.[28]

An alternative classification of NMs is according to the source of energy employed to produce their movement.[29] Accordingly, NMs can be categorized into chemically powered NMs that convert energy from the surrounding media (fuel) through chemical reactions, and physically-driven NMs that can be propelled using light,[30] or externally applied electric,[31] magnetic,[32] or acoustic fields.[21b,33] Regardless of this division, they share a main requirement: a continuous supply of energy is necessary to endure their movement. In the context of our central theme, nano/micromotor-driven SERS, three kinds of NMs have started to be studied: chemical, electrical, and magnetically propelled NMs.

The following sections brief the main characteristics of these propulsion systems and the yield movement capabilities that they offer. Information for other propulsion systems as acoustically propelled, and light-driven NMs can be found in more detail at the following references.[34]

2.1. Chemical, Electrical, and Magnetic Nano/Micromotors

Chemically driven NMs generate movement due to chemical reactions that occur between the NMs surface and the surrounding media (**Figure 1A**). In order to do this, chemical-powered NMs include sites with metallic surfaces such as Pt,[35] Ni,[36] or Mg, as well as biological enzymes,[37] in which the reaction with the fuel can take place. Because the result of this reaction will determine the speed, the components working as engines, are selected based on the required application. With this into account, the NMs can be tailored to navigate toward regions with high fuel concentration,[38] or different pH,[39] though usually requiring an additional directing tool such as a magnetic field. The most commonly employed reaction in chemical NMs is the decomposition of H_2O_2.[40] This reaction has been thoroughly studied because propels the NMs through three possible mechanisms: self-electrophoresis, bubble propulsion,[41] or self-diffusiophoresis.[42] In self-electrophoresis propulsion (Figure 1A), the generated protons travel to the cathode and develop an asymmetric electric field. The self-generated potential causes an electroosmotic flow by proton migration in the electrical double layer of the swimmer.[35,43] For the bubble propulsion (Figure 1A) the detachment of microbubbles of the decomposition products (O_2) moves the NMs in opposite directions.[41] Finally, the self-diffusiophoresis propulsion (Figure 1A) can be considered a minor scale propulsion of the bubble propulsion. The products are unable to produce a bubble to recoil, however, the instantaneous concentration gradient creates a pressure gradient that propels the NM.[42] H_2O_2 fuel is the most employed but since considered as non-biocompatible, other reported fuels include glucose,[44] or urea.[45]

Magnetically driven NMs use magnetic fields as the main source of energy to produce movement (Figure 1B). Their structure incorporates a magnetic constituent made of metallic Ni,[46] Fe,[47] Co,[48] its alloys,[49] or oxides[50] that react in response to an applied magnetic field gradient or to a time-dependent magnetic field. The direction, intensity, time, and/or position dependency of the external field applied determines the final movement of the magnetic NMs. According to the resulting movement, the magnetic NMs can be categorized into five main motions: linear displacement, corkscrew, wagging, surface-assisted, and spinning motion. The simplest case of translational manipulation of magnetic NMs implies the balance of the Stokes drag and the magnetic force exerted by a magnetic field gradient alone, with no fluid stream but just the Brownian diffusion, considering in this case a linear magnetophoresis (Figure 1B-a).[50–51] The corkscrew motion is produced by an external rotating magnetic field on magnetic NMs with helical structures (Figure 1B-a).[18b] The applied field produces a rotation of the NMs along its central axis, which results in translational motion that can be regulated with the frequency of rotation of the magnetic field. The direction of movement can be easily inverted with a field rotating in the opposite direction, while the orientation can be controlled by uniform fields. Wagging motion (Figure 1B-a) is commonly found in flexible magnetic NMs that can be deformed under an oscillating magnetic field.[52] Under the oscillating field, the magnetic parts bend the body in a non-reciprocal configuration to produce a small caudal that propels the NMs.[52a] The required flexible body can be obtained using a premade

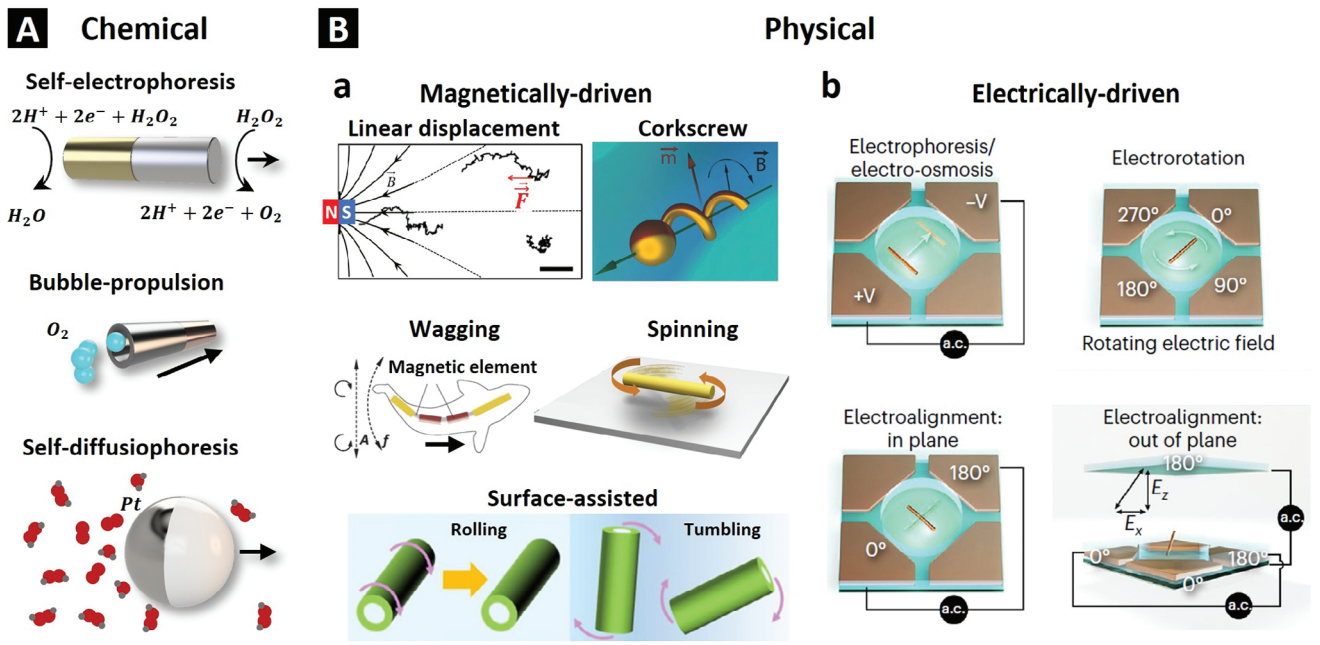

Figure 1. Alternatives for controlled movement at the micro/nanoscale using NMs. A) Chemically driven NMs. The decomposition of H_2O_2 illustrates three possible mechanisms to produce movement: self-electrophoresis,[35,43] bubble propulsion,[41] or self-diffusiophoresis.[42] B) Physically driven NMs. B-a) Diagrams of the five main motions in magnetically driven NMs: linear manipulation, corkscrew, wagging, spinning, and surface-assisted (rolling and tumbling). B-b) Electrokinetic effects for transport and orientation using electric tweezers. (A) (self-electrophoresis) Adapted with permission from ref.[35] Copyright 2004, American Chemical Society. (bubble propulsion) Adapted with permission from ref.[41] Copyright 2016, The Royal Society of Chemistry. (self-diffusiophoresis) Adapted with permission from ref.[42] Copyright 2011, American Chemical Society. (B-a) (Linear manipulation) Adapted with permission from ref.[50] Copyright 2017, American Chemical Society. (Corkscrew) Adapted with permission from ref.[61] Copyright 2018, Wiley-VCH. (Wagging) Adapted with permission from ref.[52a] Copyright 2016 Wiley-VCH. (Spinning) Adapted with permission from ref.[53c] Copyright 2022, Elsevier. (Surface-assisted) Adapted with permission from ref.[55] Copyright 2022, Elsevier Ltd. (B-b) Adapted with permission from ref.[60] Copyright 2023, The Author(s), under exclusive license to Springer Nature Limited.

structure of flexible polymers[49b] or using multiple rigid segments linked by hinges.[52d] The spinning motion of NMs (Figure 1B-a) occurs when the applied magnetic fields are unaligned with the magnetic momentum of the NMs, so it produces a torque that initiates the rotation. It is often overlooked since usually does not produce a translational net motion like the previously discussed. Despite this initial overlook, it has shown improvements in the loading and releasing of molecules since the NM behaves as a micro stirrer.[53] Surface-assisted motion occurs when magnetic fields are applied on NMs in the proximity of surfaces. The presence of the boundary produces a propulsion gradient in the NMs that results in their displacement.[54] These NMs are commonly referred to as surface -walkers, as their movement is in a rolling or tumbling fashion over the surface (Figure 1A-d).[55] Surface-walkers have shown capabilities of movement through rough surfaces and slopes,[56] and even been able to move on vessel-like walls against physiological flows.[57] In contrast with chemical NMs which can only move randomly in environments with high enough fuel concentration, magnetically driven NMs can move in a wider range of mediums, and be manipulated at a distance and with a guided direction.[58]

Electric fields are another option to control the movement of NMs (Figure 1B-b). As small particles are suspended in a liquid media, NMs are susceptible to the appearance of electrokinetic phenomena, as electrophoresis and dielectrophoresis forces that can be used to produce movement.[59] Electric tweezers use these forces in an effective manner to control the movement of the NMs.[31] Normally DC and AC electric fields are used to manipulate the NMs, producing linear displacements through electrophoresis, spinning or electrorotation, and alignment in planar and 3D orientations.[60]

2.2. Fabrication of NMs with Noble Metal Surfaces for SERS Sensing

To endorse the nanomotors (NMs) with the SERS functionality, they must have an accessible plasmonic surface. There are four well-documented strategies to achieve this: vapor-phase deposition of plasmonic materials; in situ growth of plasmonic nanoparticles; utilization of rolled-up plasmonic tubes; and the direct application of NPs as NMs. Interestingly, numerous reports highlight NMs featuring surfaces made of noble metals like gold and silver.[62] These metals are particularly significant because of their inherent plasmonic properties. This section provides a comprehensive review of various methods employed in fabricating NMs with such surfaces and, where applicable, their integration with SERS sensing (**Figure 2**).

Electrodeposition is a well-known technique in the synthesis of NMs (Figure 2A).[63] This preparation method is usually assisted by a sacrificial porous template of rack-etched polycarbonate or anodized alumina. The synthesis occurs in the inside of the

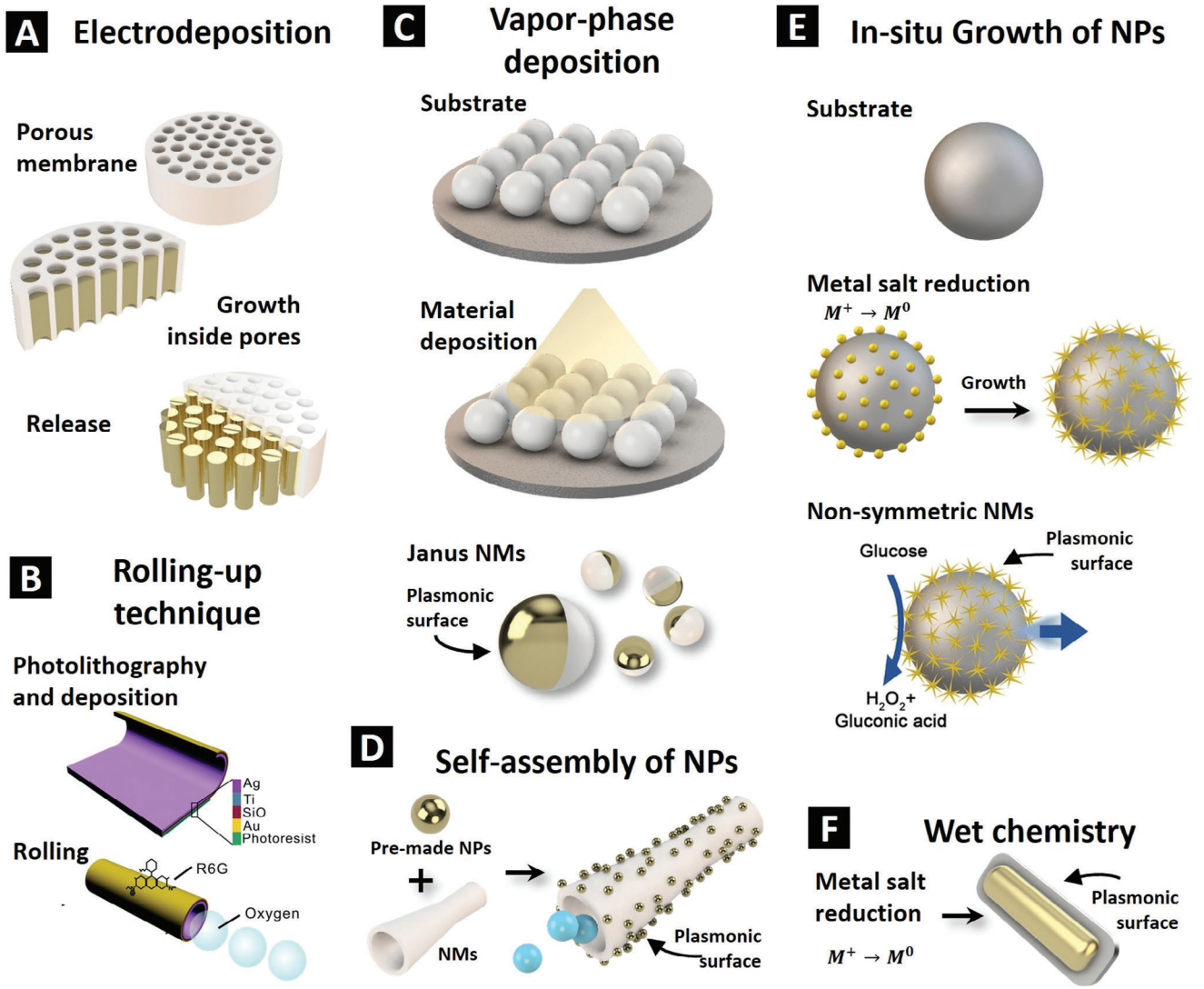

Figure 2. Representative strategies to produce NMs with noble metal surfaces. A) Diagram of the electrodeposition method. The NMs grow inside the pores of a sacrificial membrane for posterior release. B) Rolling-up technique. The difference in stress forces of the different layers produces the deformation into tubular/spiral structures. C) Vapor-phase deposition coats an existing substrate with multiple materials. D) Self-assembly of NPs on NMs´ functionalized surface. E) In situ growth of NPs involves the reduction of a metal salt that nucleates onto the surface of the NMs. F) The direct use of NPs as NMs benefits from its smaller size, which makes them attractive for applications as internalization inside cells. (A) Adapted with permission from ref.[65] Copyright 2015, American Chemical Society. (B) Adapted with permission from ref.[69] Copyright 2016, The Royal Society of Chemistry. (C) Adapted with permission from refs.[16,72a] Copyright 2020 Wiley-VCH and 2022 Elsevier Ltd. (D) Adapted from ref.[74] with permission from The Royal Society of Chemistry. (E) Adapted with permission from ref.[76] Copyright 2023, The Royal Society of Chemistry 2023. (F) Adapted with permission from ref.[77] Copyright 2019, Wiley-VCH.

porous, thus, limiting the growth of material within a desired diameter (given by the template) and growing vertically filling the pore. The membrane is then dissolved to free the NMs. Three main morphologies are regularly obtained from this method: wires, tubular structures, and helical shapes. Wire-like NMs can be constructed as a single body or through the sequential growth of different segments. Sequential growth can be used to create chemically propelled NMs by using two different metals or by adding direction control capabilities due to the inclusion of a nickel segment.[46b] Tubular NMs normally use membranes with conical-shaped pores and conducting polymers that grow on the surfaces mimicking the conical shape. Subsequently, an internal magnetic layer can be deposited in a posterior step.[64] For helical shapes, the codeposition of metals and posterior etching result in the formation of nanohelices.[65] This production method allows batch production of NMs and can be reproduced with relative facility. However, special attention must be taken when working with multisegment NMs, due to possible suboptimal adhesion between segments that could result in brittle joints.[66]

Electrodeposition-derived nanomotors have interesting potential as SERS platforms, although their use in this context has not been explored yet. The process of electrodeposition can create

noble metal surfaces quickly, and the surfaces produced are typically relatively clean, which is advantageous for SERS applications.[46b]

A rolled-up fabrication technique takes advantage of differentially strained layers that fold due to stress relaxation to create tubular or spiral structures.[67] The functional layers that form the NMs are deposited over a sacrificial patterned template that is removed and triggers the rolling process. This method has been used to produce tubular NMs with external plasmonic surfaces (Figure 2B) and SERS sensing capabilities.[68] Indeed, the tubular structure shows a much better SERS signal compared to the flat surface before the roll-up.[68] This increase can be attributed to the curvature that modifies the surface plasmonic resonance frequency or more likely, to the formation of irregular nanostructures in the surface during the rolling process.[68,69] Two interesting findings should be emphasized. First, the increase in the thickness of the plasmonic NMs is detrimental to the SERS signal, which highlights the nanoscale nature of the SERS signal.[69] Second, the increase in the movement rate of the NMs within the solution increases the collection of the analyte because of the increased diffusion.[70] Interestingly, it has also been reported that chemical nanomotors often do not reach a plateau condition, likely due to the presence of the fuel or because high-speed movement is not conducive to the attachment of molecules.[69] In summary, rolled-up fabrication allows the fabrication of SERS active NMs, with control over the diameter and length as well as a variety of materials to use. Nevertheless, the common use of photolithography to form the initial pattern of the sacrificial layer can decrease the appeal of this technique.

Vapor-phase deposition methods, such as sputtering or physical vapor deposition, eliminate the need for photolithography-produced patterns in the rolled-up process. In these methods, the chosen material is deposited onto the substrate's exposed surface, simultaneously protecting the bottom and forming a thin layer on the opposite side (Figure 2C). This approach is particularly efficient for creating Janus particles and can be adapted for more complex coatings. By manipulating the substrate orientation (using techniques like glancing angle deposition, GLAD, or dynamic shadowing growth), structures with varying exposed areas of multiple metals can be achieved.[71] Such versatility has enabled the production of Janus NMs suitable for SERS measurements of H_2O_2 concentration in cellular microenvironments.[72] In addition to Janus particles, this method can also coat other pre-fabricated structures, like helical structures[46a] or biotemplates.[73] While these techniques typically produce rougher surfaces favored for SERS sensing, a more uniform coating is preferred when using specific patterned templates.

Another family of techniques to achieve the synergy between NMs and SERS convenes the use of plasmonic NPs. Self-assembly of NPs over NMs is possible using functional groups with high affinity for the NPs in the NMs surface (Figure 2D). This approach has been demonstrated using thiol groups such as (3-mercaptopropyl) trimethoxysilane.[74] or thiolated polymers[75] but not yet studied for NM-driven SERS applications. The growth of plasmonic NPs is the most used approach to obtain NMs with SERS capabilities (Figure 2E). This method consists of the reduction of a metal salt onto the surface of the NMs such as silica coatings or magnetic beads. The NPs produced can be varied in materials and morphology,[76] depending on the reduction conditions. Finally, the direct use of nanoparticles as nanomotors has been reported to yield significant advances within the field, NMs made of Au@Ag core-shell nanorods (NRs) have been proposed for the detection of explosives.[77] However, given the fact that the molecule of interest presents a low SERS intensity, the use of these chemical propelled NMs was designed to consider the presence of the fuel used in the SERS spectra. Hydrogen peroxide is, as a matter of fact, a good example, showing a Raman signal ≈877 cm^{-1}.

The current fabrication of nanomotors with SERS capabilities primarily focuses on leaving a free plasmonic surface for close contact with the analyte. This approach is certainly appropriate since SERS is a proximity effect. However, it is worthwhile to consider the fabrication of nanomotors that include optical accumulators such as MOFs or mechanical traps,[78] which can increase the concentration of the analyte near the plasmonic surface. Notably, mechanical actuation responding to parameters like pH or temperature are strategies found in both fields, suggesting potential synergy when combined. Regarding the use of nanoparticles (NPs), most research involves silver colloids. An interesting alternative could be gold nanoparticles, offering a wider range of morphologies for exploration. A significant addition is the compatibility of plasmonic structures with photothermal therapy, adding extra functionalities to SERS-capable nanomotors.[72a] Nonetheless, cytotoxic effects have been observed in metallic NPs,[81] so special emphasis should be placed on subsequent studies for biological applications.

3. Nano/Micromotor-Driven SERS

NMs with plasmonic surfaces can be used directly to produce an SERS signal. This approach is commonly referred to as direct sensing and has been proved in preliminary works that used rutinary SERS targets such as rhodamine 6G (R6G) or Nile blue.[69] Nevertheless, depending on the analyte to be detected, three main problems are to be addressed for the correct use of NMs-driven SERS: low affinity to the surface, small cross-section, and different contributions in samples with multiple analytes.

3.1. Increase of the NM-Driven SERS Sensitivity and Selectivity

The most common way to increase the intensity of the SERS signal is through the formation of electromagnetic hot spots. The formation of hot spots using aggregates is the classical approach to increasing the SERS signal. The in situ growth of NPs through the reduction of Ag ions with PVP ions in wire nanomotors coated with porous silica illustrates the formation of hot spots inside gaps (**Figure 3**Aa).[82] The silica coating offers empty spaces that were performed using embedded PS beads that were posteriorly dissolved. In such sites (Figure 3Ab), the synthesized Ag NPs (green) are nearby, resulting in an increase of the SERS signal of the R6G. An optical image with the corresponding SERS map is presented (Figure 3A-c,e), showing the uniformity of the material. One advantage of this procedure is that silica surfaces with complex morphologies can be uniformly coated with NPs.[83] Moreover, the remaining free space can be

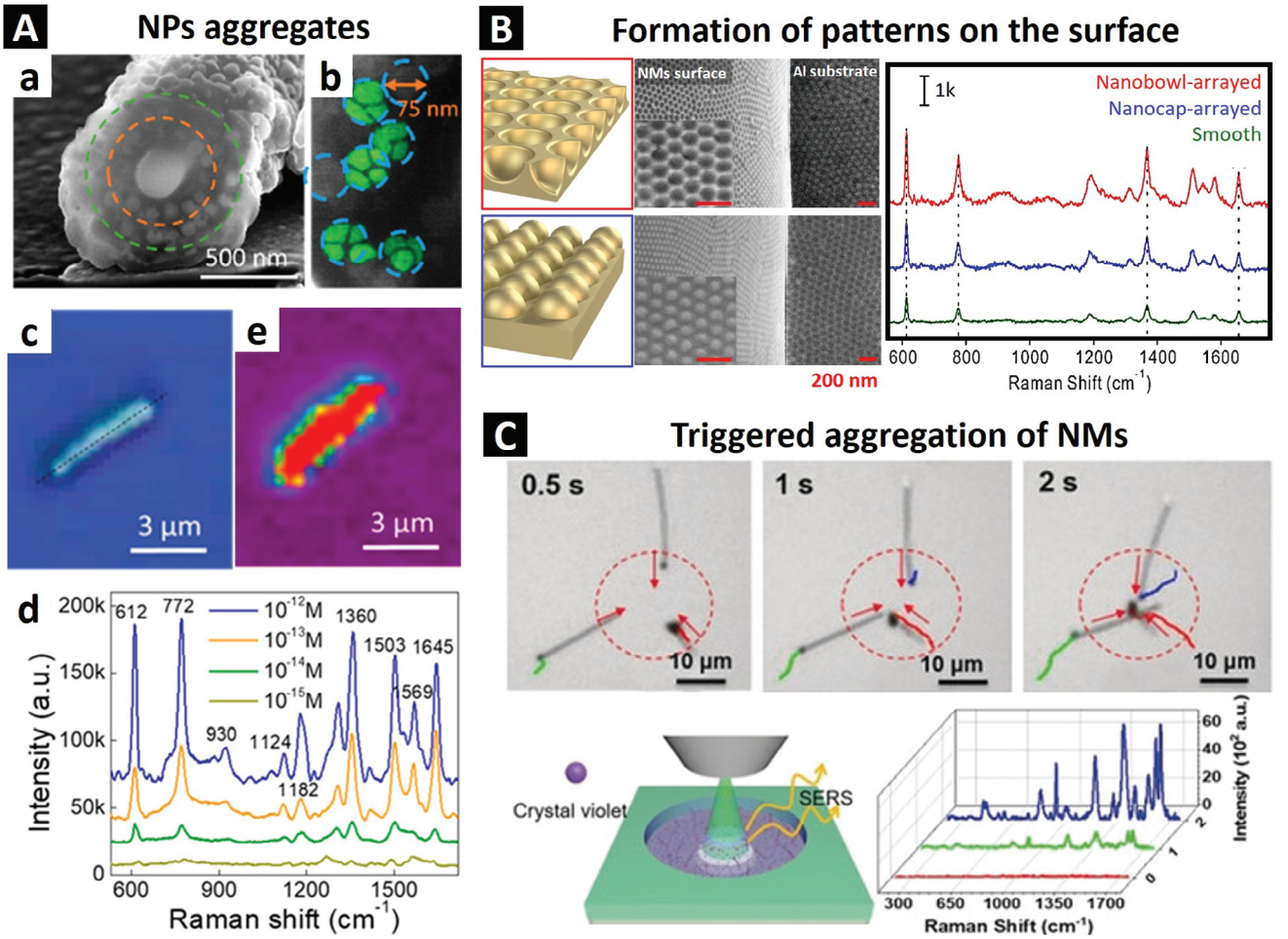

Figure 3. Common strategies to increase the NM-driven SERS sensitivity. A) Synthesis of NP aggregates on wire NMs. A-a) Cross-section of NMs covered by a silica shell and NPs embedded in the cavities. A-b) Close up of the cavities, in green the silver NPs. A-c) optical image of the NMs and (A-e) SERS mapping of the NMs showing a uniform enhancement. A-d) SERS spectra of R6G using different concentrations. B) Different superficial patterns in NMs to increase the SERS signal: nanocap (blue) and nanobowl (red). Diagram and corresponding SEM images. SERS spectra of R6G were acquired from the different patterns compared with a smooth (green) surface. C) Top: time-lapse of the induced aggregation. Bottom: Schematic of the SERS detection process and the corresponding SERS spectra of the time-lapse intervals showing the increasing intensity with the proximity. (A) Adapted with permission from ref.[82b] Copyright 2018, America Chemical Society. (B) Adapted with permission from ref.[70] Copyright 2020, America Chemical Society. (C) Adapted with permission from ref.[20b] Copyright 2018, Wiley-VCH.

used for the cargo and subsequent release of different molecules, while at the same time, the nearing NPs yield a SERS signal for the monitoring of the concentration (Figure 3A-d). Another way to create hot spots is the use of patterns on the surface of NMs. Figure 3B shows magnetically driven NMs with a pattern on the surface for direct SERS sensing.[70] Two patterns were studied: nanobowl and nanocap-arrayed with concave and convex structures respectively. Compared with plane NMs, the two explored patterns, show an increase in the strength of the signal. These nanomotors take advantage of the generation of controlled gaps that result in hot spots for sensing. Finally, an elegant way to increase the SERS signal relies on the creation of aggregates upon a trigger stimulus (i.e., the presence of the analytical target or an external trigger on the motion of the NMs).[22b,84] This behavior creates on-demand hot spots between the NMs and increases the SERS signal of molecules on the surface. Figure 3C shows the light-triggered aggregation of chemically propelled match-like NMs.[20b] The NMs exhibit positive phototaxis, with motion directed by a focused UV beam, such that the new aggregate produces a stronger SERS signal of CV. This aggregation behavior of NMs can also be produced by chemical,[85] ultrasound,[86] or magnetic stimuli,[87] offering a possible alternative for new SERS substrates. Overall, this triggered aggregation process can be reversible and improves the detection of analytes with small cross-sections. Alternatively, hot spots can also be produced on single particles with sharp tips such us stars, wires, or cubes in which the electric field is concentrated mainly at the apexes of their tips. The use of these structures may lead to plasmonic nanomotors with smaller dimensions.

In the case of analyte selectivity, this parameter can be greatly enhanced through the use of chemosensors. Chemosensors are molecules with high SERS cross-sections that are highly selective for specific molecules or families of molecules. For instance, 3-mercaptophenylboronic acid has been utilized as a

chemosensor on gold-coated Janus nanomotors to quantify locally available H2O2.[72a] In this scenario, the boronic acid is oxidized by hydrogen peroxide, producing 3-hydroxythiophenol.[88] This reaction alters the SERS spectrum of the boronic acid, introducing a new band at 882 cm^{-1}, which can be used to quantitatively monitor peroxide concentration in the range of 100 nM to 10 µM. Furthermore, the interaction of chemosensors with analytes for indirect sensing can also be reversible, allowing for continuous monitoring. As an example, the detection of mercury (Hg) in water can be monitored using 4-mercaptopyridine.[89]

3.2. Effects of the Motion for NM-Driven SERS

One interesting aspect of combining SERS spectroscopy with NANOMOTORS is the molecular enrichment of the sensing surface caused by the mechanical movement of the NMs. The movement of the NMs in a solution increases the SERS signal due to the enhanced diffusion and consequent acceleration of the process of molecular adsorption.[70] The function of the mini stirrer resulting from the movement of the NMs increases the compatibility between these technologies, while also increasing the detection speed. **Figure** 4A shows the direct comparison of static (green) and active magnetically driven NMs.[70] While inactive NMs are left in the solution for the normal diffusion and adsorption process (Figure 4A-a), the active ones are subjected to an external rotating magnetic field that produces drifting trajectories. Figure 4A-b presents an optical image of the trajectory followed by the NMs, and a schematic of the rotational movement. The direct comparison between the active and inactive NMs that are placed during 15 min in the solution shows a 2.1 times major increase in the intensity for the active NMs than the static (Figure 4A-b). The close examination of the characteristic peaks in Figure 4A-c is put in a histogram in Figure 4A-d. This molecular enrichment effect is further improved when physical traps[78] are used to encapsulate the analyte, for example, with an exterior layer of diatom that serves as a structural trap for the detection of different analytes.[82b] Similar results are reported with porous silica coatings.[82]

A curious synergistic effect is also reported resulting from the rotational movement: the re-usability of NMs as SERS substrates. Figure 4B shows magnetic NMs made of three aligned magnetic beads coated with silica.[53b] The shell is functionalized with Ag NPs to produce the SERS signal. A microfluidic array was employed to show that these NMs have translational and rotational motion. Their magnetic attiring increases the accumulation of R6G (Figure 4B-a), while the rapid rotation in a clean environment decreases its signal, thus acting as a washing setup for reuse (Figure 4B-b). This reuse was demonstrated by translating the NMs to a CV-rich environment and obtaining the corresponding SERS signal (Figure 4B-c). This apparent contradiction, between an increase in the detection and the cleaning process, both consequence of the rotation movement, could be explained considering the concentration of the environment of the NMs, the weak interaction between the analytes, and the rotation speed that promotes the diffusion to one side or the other.

Molecular enrichment is the most explored outcome of integrating SERS in nanomotors. This effect enables faster analysis and an enhanced limit of detection, thanks to the stirring behavior of the nanomotors. Commonly, this is compared to magnetic stirring bars, leading to the popular use of magnetic NMs in conjunction with SERS, often preferred over other propulsion methods. Alternatively, magnetic control can be combined with different propulsion methods. However, the comparison with the rotational movement of stirring bars has its limitations. For example, it has been demonstrated that up-and-down oscillations in 3D space can also facilitate molecular enrichment.[76]

3.3. NMs-Driven SERS Applications

SERS applications may be broadly divided into detection and imaging. The combination with the spatially controlled movement of NMs offers the possibility to perform biological detection at the inter and intracellular levels. **Figure** 5A illustrates the detection at the intercellular level, by sensing metabolites in the vicinity of an *E. coli (Escherichia coli)* bacteria using SERS-capable NMs.[60] Here an electrically-driven Au-wire nanomotor coated with silica and Ag NPs is used to monitor the vicinity of the bacteria and their produced metabolites. Three moments are emphasized: prior to the contact with the target (20 µm distance), where no signal is recorded; at contact within the probe and the target, which results in a SERS spectrum; and, finally, the separation (15 µm), where the signal vanishes with time. This experiment offers evidence of the capacity of SERS active nanomotors to generate location-specific SERS signals from a target. Also, the controlled positioning and orientation in space could be useful to monitor different areas of interest over the cell surface.

SERS nanomotors preserve their motion capabilities when internalized inside cells. As an example, Figure 5B shows a schematic illustration for targeted SERS sensing of intercellular sites on HeLa cells with chemically propelled magnetic-guided NMs.[76] The sensing platform gets inside the cell membrane with the help of an induced glucose concentration increase in the culture medium to increase the cellular uptake. After internalization, the SERS nanomotors, which preserve their magnetic control, can be aggregated when desired to increase the electric field and induce a larger enhancement factor. Notably, direct analysis by SERS inside cells can be a difficult task because of the complex internal cell environment; for example, vibrational signals of HeLa cells are multiple[83,90] and can overlap and even hide the signals of the analyte under study. In such a case, the best alternative is the use of one or more chemosensors to selectively monitor the analytes under study. Furthermore, it is possible to study undergoing mechanisms or chemical processes inside cells using different targets. For instance, cytochrome C release and cellular pH change have been simultaneously monitored through SERS using aptamers (cytochrome c-specific) and 4-mercaptobenzoic acid, respectively.[91] In addition to the phagocytosis process of internalization, magnetic helical nanomotors capable of membrane penetration and SERS sensing have been reported.[92]

The monitoring of molecule release has also been a subject of research. In this context, while mechanical supports like silica coatings, dendritic structures, or other forms of cages can be utilized for drug delivery applications, the combination of magnetic nanomotors and SERS can offer more controlled behavior. In this setup, the mechanical movement can be precisely used to determine the ratio and distribution of released molecules in

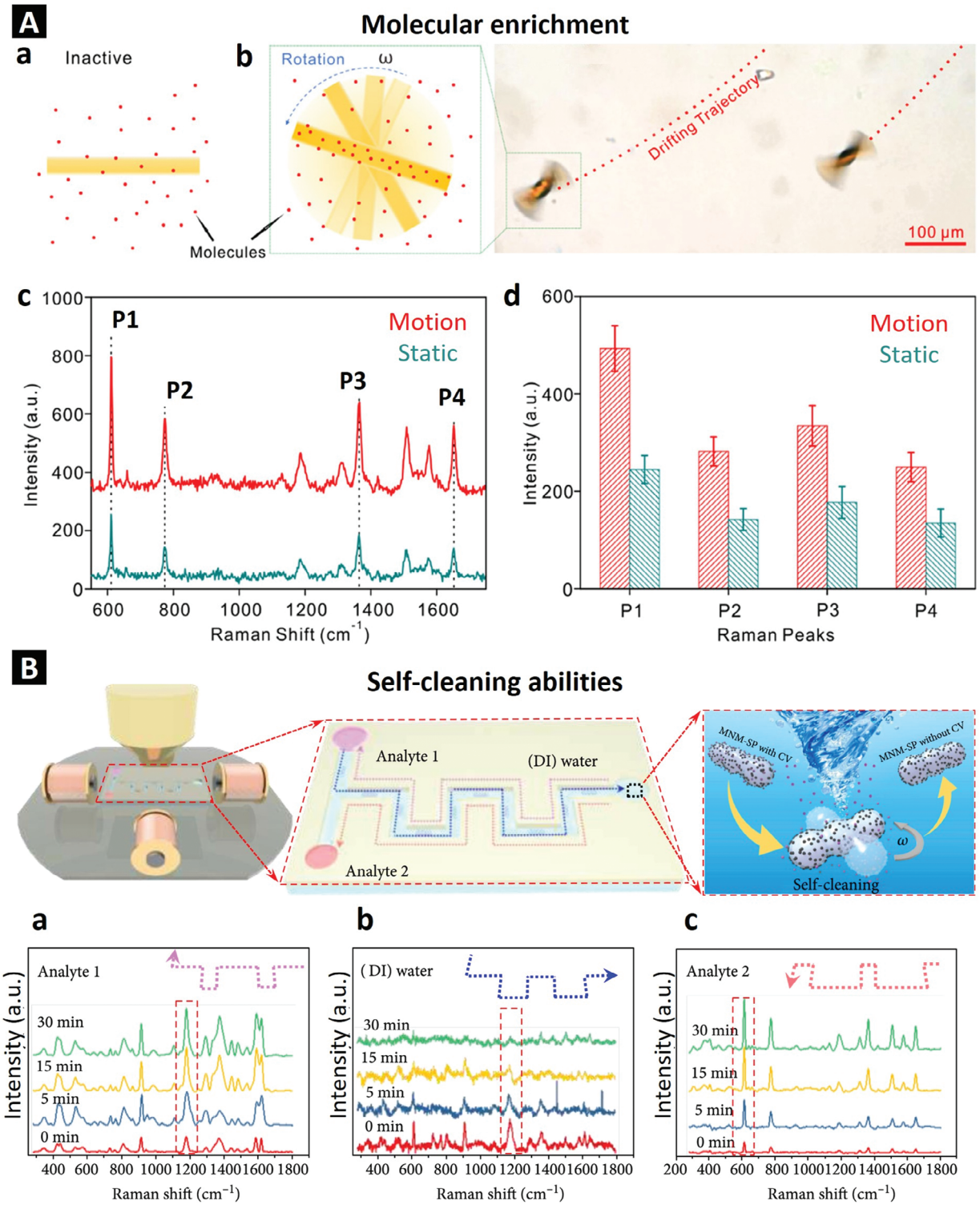

Figure 4. Effects of the motion for NM-driven SERS. A) Molecular enrichment due to the movement of the NMs. A-a) Diagram of the absorption process with non-motile NMs. A-b) Optical image of the trajectory of the NMs, the inset is a diagram of the oscillation that promotes the acceleration in the absorption process. A-c) Comparison of the SERS signal between both NMs: with and without movement (red and green, respectively). A-d) Comparison of the intensities for each peak mark in Ac. B) Cleaning abilities for NMs sensing non-covalent analytes. B-a) Schematic of the experimental setup. B-b) First travel to analyte one within 30 min. Second travel to the cleaning station. B-c) Final travel to the second analyte within 30 min. The corresponding SERS spectra demonstrate the reusability of the NMs for SERS measurements. (A) Adapted with permission from ref.[70] Copyright 2020, America Chemical Society. (B) Adapted with permission from ref.[53b] Copyright 2020 Yong Wang et al. Exclusive Licensee Science and Technology Review Publishing House. Distributed under a Creative Commons Attribution License (CC BY 4.0).

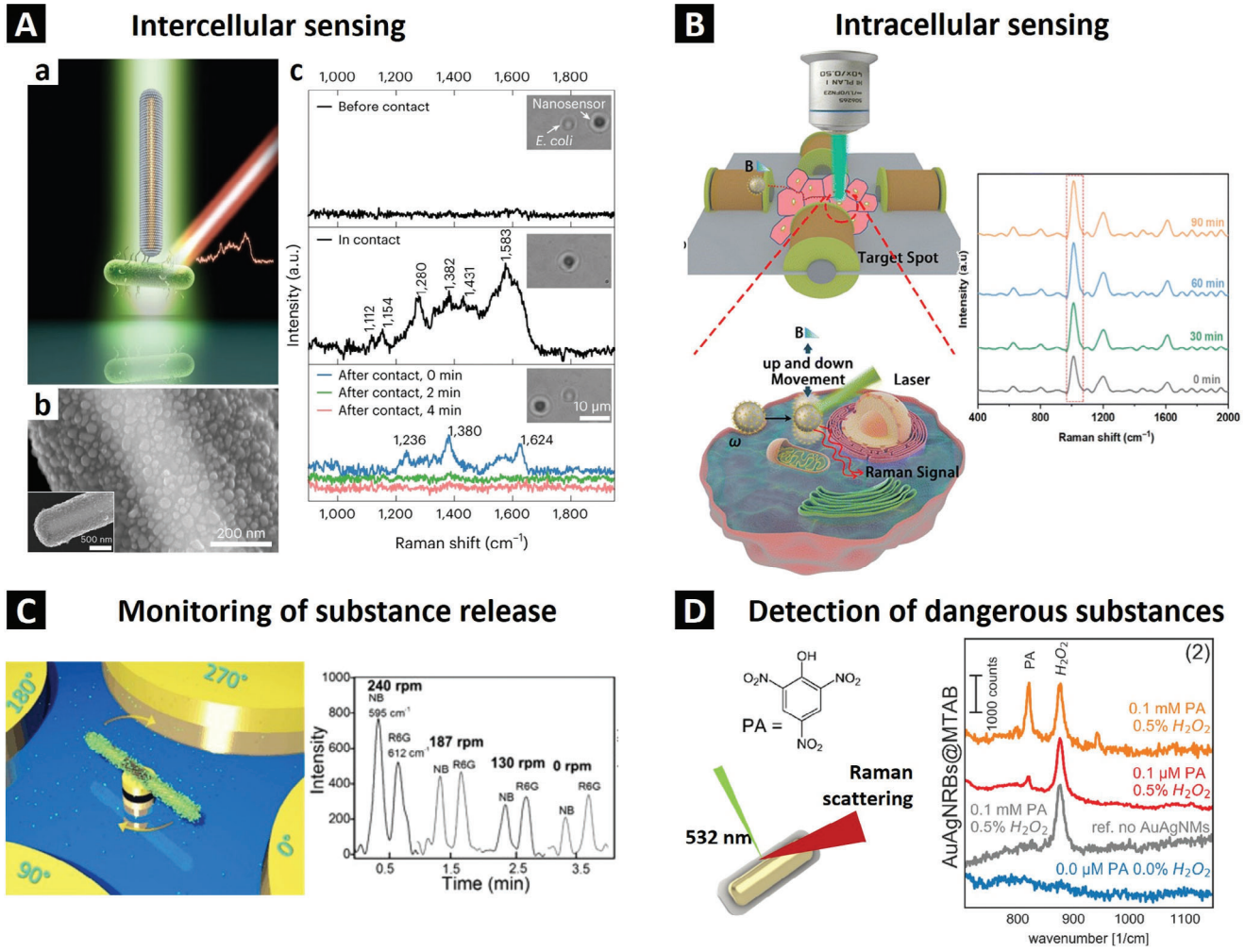

Figure 5. Detection applications of NM-driven SERS. A) Intracellular sensing in the vicinity of a *E.Coli* bacteria. A-a) Conceptual image of the NM sensing in the proximity of the bacteria. A-b) SEM image of the NMs surface showing Ag NPs aggregates. A-c) Evolution of the SERS signal when the NM is approaching the bacteria and then leaving. B) Schematic illustration of chemically propelled magnetic-guided nanomotor for intracellular SERS sensing. Evolution of the Raman signal at 1007 cm^{-1} applying the oscillating magnetic field. C) Schematic of rotating NMs controlled by electric tweezers, that monitor the release of molecules. Representative SERS intensity of characteristic peaks of Nile Blue and R6G showing the different release rates. D) Au@Ag NMs for detection of dangerous substances Left: Scheme of core-shell rod NMs for direct sensing of explosives. Right: SERS spectra detection of picric acid at 820 cm^{-1} and H_2O_2 at 877 cm^{-1}. (A) Adapted with permission from ref.[60] Copyright 2023, The Author(s), under exclusive license to Springer Nature Limited. (B) Adapted with permission from ref.[76] Copyright 2023, The Royal Society of Chemistry. (C) Adapted with permission from ref.[93] Copyright 2015, Wiley-VCH. (D) Adapted with permission from ref.[77] Copyright 2019, WileyVCH.

the environment. Simultaneously, the spectral signal can be employed to monitor the remaining concentration within the NMs in almost real-time. This approach was illustrated in Figure 5C, where electrically-driven NMs were used for monitoring the controlled release of multiplex biochemicals.[93]

A final example of using nanomotors and SERS is in detecting molecules such as pollutants or biomolecules like DNA[94] in liquid environments. Traditionally, the use of NMs in this area has relied on changes in their movement due to the presence of various contaminants.[95] However, this method lacks the ability to specifically identify pollutants in real-world scenarios. Additionally, numerous uncontrollable factors can alter the motion of the sensor motors. Therefore, incorporating SERS spectroscopy can enhance the use of NMs by enabling precise identification of pollutants and their concentration. While it is possible to use NMs to navigate through media to capture pollutants, which are then collected for later analysis,[96] in situ measurement on the NMs is much more promising. As an illustration of this sensing application, Figure 5D shows chemically-propelled Au@Ag core-shell nanorods acting as an optical sensor for detecting explosives.[77]

4. Conclusion and Outlook

The integration of nano/micromotors (NMs) with surface-enhanced Raman scattering (SERS) spectroscopy constitutes a promising and relatively unexplored area of research, brimming with potential for innovation. Preliminary studies have underscored the ability of SERS-active NMs to offer remote feedback

regarding the local environment. Additionally, these investigations demonstrate the potential to achieve molecular enrichment on the sensing surface. This enrichment is ascribed to the mechanical movement of the NMs, which also maintains precise control over movement at the nano/micro scale. The current applications of SERS integrated with nanomotors are primarily confined to the direct detection of analytes in simplistic solutions.[70] However, the landscape of this field is rapidly evolving, thanks to significant advancements in both detection methodologies and instrumental enhancements.

One of the primary challenges in the application of SERS with nanomotors is the complexity of matrix solutions. In highly complex fluids, especially those of biological,[13] or natural origin,[97] the intrinsic composition often obstructs or inhibits the observation of characteristic SERS signals of the target analyte. Indirect SERS methods have emerged as a solution, leveraging the functionalization of plasmonic surfaces with molecules that possess a large SERS cross-section and high affinity for the analyte (chemosensors).[98] Magnetic nanomotors, in particular, offer promising prospects. They can explore a large volume of sample with minimal quantities, reacting with corresponding analytes and concentrating the nanomotors in a small spatial region for comprehensive SERS analysis without producing interferences in the signal.[99] The potential for sensor recycling and reusability through magnetic manipulation amplifies the efficiency and applicability of this technology.[53b] Furthermore, SERS can transform nanomotors into encoded nanoparticles,[100] expanding their utility in detecting and identifying viruses,[101] bacteria,[102] and eukaryotic cells,[103] and in tissue imaging.[104] The advent of SERS widefield microscopy[105] has accelerated these processes, enabling rapid and efficient analysis.

Also, intracellular studies of metabolic reactions;[106] are another frontier being explored, with nanomotors promoting the accumulation of SERS inside the cells[107] and positioning them beside target organelles.[61] Real-time monitoring of these processes can be now achievable through SERS holography,[108] and when combined with the magnetic generation of heat (magnetothermia), applications extend detection/quantification to drug release and selective cell killing.[32] The utilization of nanomotors offering SERS responses, and simultaneously promoting photocatalysts, represents another potential improvement.[109]

In summary, the synergy between SERS and nanomotors is poised to transcend existing boundaries. By transporting SERS substrates to designated locations, nanomotors facilitate in situ and real-time analysis of complex chemical and biological samples. This integration is set to revolutionize healthcare, environmental science, and material engineering, heralding a new epoch in detection, quantification, and bioimaging. Enhanced sensitivity, specificity, and versatility are anticipated, driving innovations that will address contemporary challenges and unveil new opportunities in analytical science.

Acknowledgements

This work was supported by the projects PID2020-120306RB-I00 and PID2020-119242-I00 (funded by MCIN/AEI/10.13039/501100011033), PDC2021-121787-I00 (funded by MCIN/AEI/10.13039/501100011033 and European Union Next Generation EU/PRTR), 2020SGR00166 (funded by Generalitat de Cataluña), 2021PFR-URV-B2-02 (funded by Universitat Rovira i Virgili), and by the European Union Horizon 2020 Research and Innovation Program under the H2020 Marie Sklodowska-Curie Actions, grant number 872233 ("PEPSA- MATE").

Conflict of Interest

The authors declare no conflict of interest.

Keywords

nano/micromotors, SERS, spatially controlled sensing

Received: November 29, 2023
Published online:

[1] E. Lauga, T. R. Powers, *Rep. Prog. Phys.* **2009**, *72*, 096601.
[2] R. P. Feynman, *Resonance* **2011**, *16*, 890.
[3] M. Zarei, M. Zarei, *Small* **2018**, *14*, 1800912.
[4] A. Aziz, S. Pane, V. Iacovacci, N. Koukourakis, J. Czarske, A. Menciassi, M. Medina-Sánchez, O. G. Schmidt, *ACS Nano* **2020**, *14*, 10865.
[5] a) J. A. Tejeda-Rodríguez, A. Núñez, F. Soto, V. García-Gradilla, R. Cadena-Nava, J. Wang, R. Vazquez-Duhalt, *ChemNanoMat* **2019**, *5*, 194; b) M. Medina-Sánchez, L. Schwarz, A. K. Meyer, F. Hebenstreit, O. G. Schmidt, *Nano Lett.* **2016**, *16*, 555.
[6] J. C. Breger, C. Yoon, R. Xiao, H. R. Kwag, M. O. Wang, J. P. Fisher, T. D. Nguyen, D. H. Gracias, *ACS Appl. Mater. Interfaces* **2015**, *7*, 3398.
[7] M. A. Ramos-Docampo, P. Hurtado, A. B. Dávila-Ibáñez, R. Piñeiro, M. L. Fanarraga, V. Salgueiriño, *J. Colloid Interface Sci.* **2023**, *629*, 287.
[8] J. Parmar, D. Vilela, K. Villa, J. Wang, S. Sánchez, *J. Am. Chem. Soc.* **2018**, *140*, 9317.
[9] S. Schlücker, *Angew Chem Int Ed Engl* **2014**, *53*, 4756.
[10] G. C. Schatz, M. A. Young, R. P. Van Duyne, in *Surface-Enhanced Raman Scattering: Physics and Applications*, (Eds: K. Kneipp, M. Moskovits, H. Kneipp), Springer, Berlin, Heidelberg **2006**.
[11] J. Langer, D. Jimenez De Aberasturi, J. Aizpurua, R. A. Alvarez-Puebla, B. Auguié, J. J. Baumberg, G. C. Bazan, S. E. J. Bell, A. Boisen, A. G. Brolo, J. Choo, D. Cialla-May, V. Deckert, L. Fabris, K. Faulds, F. J. García De Abajo, R. Goodacre, D. Graham, A. J. Haes, C. L. Haynes, C. Huck, T. Itoh, M. Käll, J. Kneipp, N. A. Kotov, H. Kuang, E. C. Le Ru, H. K. Lee, J.-F. Li, X. Y. Ling, et al., *ACS Nano* **2020**, *14*, 28.
[12] R. A. Alvarez-Puebla, L. M. Liz-Marzán, *Angew. Chem., Int. Ed.* **2012**, *51*, 11214.
[13] R. A. Alvarez-Puebla, L. M. Liz-Marzán, *Small* **2010**, *6*, 604.
[14] a) V. Cupil-Garcia, J. Q. Li, S. J. Norton, R. A. Odion, P. Strobbia, L. Menozzi, C. Ma, J. Hu, R. Zentella, M. I. Boyanov, Y. Z. Finfrock, D. Gursoy, D. S. Douglas, J. Yao, T.-P. Sun, K. M. Kemner, T. Vo-Dinh, *Nanoscale* **2023**, *15*, 6396; b) S. P. Ravindranath, K. L. Henne, D. K. Thompson, J. Irudayaraj, *ACS Nano* **2011**, *5*, 4729.
[15] H. Zhong, Z. Zhang, Y. Zhou, L. Wu, P. Ke, Y. Lu, Q. Dai, X. Bao, Y. Xia, Q. Yang, X. Tan, Q. Wei, W. Xu, M. Han, L. Ma, *ACS Appl. Mater. Interfaces* **2022**, *14*, 38172.
[16] M. Valdez-Garduño, M. Leal-Estrada, E. S. Oliveros-Mata, D. I. Sandoval-Bojorquez, F. Soto, J. Wang, V. Garcia-Gradilla, *Adv. Funct. Mater.* **2020**, *30*, 2004043.
[17] A. A. Solovev, Y. Mei, E. Bermúdez Ureña, G. Huang, O. G. Schmidt, *Small* **2009**, *5*, 1688.
[18] a) G. Chatzipirpiridis, C. De Marco, E. Pellicer, O. Ergeneman, J. Sort, B. J. Nelson, S. Pané, *Adv. Eng. Mater.* **2018**, *20*, 1800179; b) L.

Zhang, J. J. Abbott, L. Dong, B. E. Kratochvil, D. Bell, B. J. Nelson, *Appl. Phys. Lett.* **2009**, *94*, 064107.
[19] a) X. Li, Y. Zhao, D. Wang, X. Du, *Colloids Surf. A* **2023**, *658*, 130712; b) M. R. Karimi, S. Khoee, B. Shaghaghi, *J Drug Deliv Sci Technol* **2023**, *80*, 104096; c) J. Shao, S. Cao, H. Che, M. T. De Martino, H. Wu, L. K. E. A. Abdelmohsen, J. C. M. Van Hest, *J. Am. Chem. Soc.* **2022**, *144*, 11246.
[20] a) X. Liu, H. Liu, J. Zhang, Y. Hao, H. Yang, W. Zhao, C. Mao, *Biomater. Sci.* **2022**, *10*, 5608; b) Y. Wang, C. Zhou, W. Wang, D. Xu, F. Zeng, C. Zhan, J. Gu, M. Li, W. Zhao, J. Zhang, J. Guo, H. Feng, X. Ma, *Angew Chem Int Ed Engl* **2018**, *57*, 13110; c) A. R. Morgan, A. B. Dawson, H. S. Mckenzie, T. S. Skelhon, R. Beanland, H. P. W. Franks, S. A. F. Bon, *Mater. Horiz.* **2014**, *1*, 65.
[21] a) J. Lv, Y Xing, X. Li, X. Du, *Exploration* **2022**, *2*, 20210162; b) A. Aghakhani, O. Yasa, P. Wrede, M. Sitti, *Proc. Natl. Acad. Sci. USA* **2020**, *117*, 3469.
[22] a) Y. Ying, A. M. Pourrahimi, C. L. Manzanares-Palenzuela, F. Novotny, Z. Sofer, M. Pumera, *Small* **2020**, *16*, 1902944; b) B. Dai, J. Wang, Ze Xiong, X. Zhan, W. Dai, C.-C. Li, S.-P. Feng, J. Tang, *Nat. Nanotechnol.* **2016**, *11*, 1087.
[23] G. A. Ozin, I. Manners, S. Fournier-Bidoz, A. Arsenault, *Adv. Mater.* **2005**, *17*, 3011.
[24] T.-C. Lee, M. Alarcón-Correa, C. Miksch, K. Hahn, J. G. Gibbs, P. Fischer, *Nano Lett.* **2014**, *14*, 2407.
[25] W. Wang, W. Duan, S. Ahmed, T. E. Mallouk, A. Sen, *Nano Today* **2013**, *8*, 531.
[26] S. Kim, S. Lee, J. Lee, B. J. Nelson, Li Zhang, H. Choi, *Sci. Rep.* **2016**, *6*, 30713.
[27] M. Fränzl, S. Muiños-Landin, V. Holubec, F. Cichos, *ACS Nano* **2021**, *15*, 3434.
[28] W. Wang, L. A. Castro, M. Hoyos, T. E. Mallouk, *ACS Nano* **2012**, *6*, 6122.
[29] M. Fernández-Medina, M. A. Ramos-Docampo, O. Hovorka, V. Salgueiriño, B. Städler, *Adv. Funct. Mater.* **2020**, *30*, 1908283.
[30] a) M. Pacheco, B. Jurado-Sánchez, A. Escarpa, *Angew. Chem., Int. Ed.* **2019**, *58*, 18017; b) J. Wang, Z. Xiong, J. Zheng, X. Zhan, J. Tang, *Acc. Chem. Res.* **2018**, *51*, 1957.
[31] D. L. Fan, F. Q. Zhu, R. C. Cammarata, C. L. Chien, *Nano Today* **2011**, *6*, 339.
[32] H. Zhou, C. C. Mayorga-Martinez, S. Pané, Li Zhang, M. Pumera, *Chem. Rev.* **2021**, *121*, 4999.
[33] T. Xu, L.-P. Xu, X. Zhang, *Appl. Mater. Today* **2017**, *9*, 493.
[34] a) M. Leal-Estrada, M. Valdez-Garduño, F. Soto, V. Garcia-Gradilla, *Curr. Robot. Rep.* **2021**, *2*, 21; b) H. Šípová-Jungová, D. Andrén, S. Jones, M. Käll, *Chem. Rev.* **2020**, *120*, 269.
[35] W. F. Paxton, K. C. Kistler, C. C. Olmeda, A. Sen, S. K. St Angelo, Y. Cao, T. E. Mallouk, P. E. Lammert, V. H. Crespi, *J. Am. Chem. Soc.* **2004**, *126*, 13424.
[36] S. B. Fournier-Bidoz, A. C. Arsenault, I. Manners, G. A. Ozin, *Chem. Commun.* **2005**, 441.
[37] A. Rodríguez-Ramos, M. A. Ramos-Docampo, V. Salgueiriño, M. L. Fanarraga, *Mater. Today Adv.* **2023**, *17*, 100353.
[38] S. Sengupta, K. K. Dey, H. S. Muddana, T. Tabouillot, M. E. Ibele, P. J. Butler, A. Sen, *J. Am. Chem. Soc.* **2013**, *135*, 1406.
[39] K. K. Dey, S. Bhandari, D. Bandyopadhyay, S. Basu, A. Chattopadhyay, *Small* **2013**, *9*, 1916.
[40] Y. Tu, F. Peng, X. Sui, Y. Men, P. B. White, J. C. M. Van Hest, D. A. Wilson, *Nat. Chem.* **2017**, *9*, 480.
[41] W. Z. Teo, H. Wang, M. Pumera, *Chem. Commun.* **2016**, *52*, 4333.
[42] S. J. Ebbens, J. R. Howse, *Langmuir* **2011**, *27*, 12293.
[43] B. Jang, M. Ye, A. Hong, X. Wang, X. Liu, D. Bae, J. Puigmartí Luis, S. Pané, *Small Sci.* **2023**, *3*, 2300076.
[44] E. M. Kutorglo, R. Elashnikov, S. Rimpelova, P. Ulbrich, J. Říhová Ambrožová, V. Svorcik, O. Lyutakov, *ACS Appl. Mater. Interfaces* **2021**, *13*, 16173.
[45] A. C. Hortelão, T. Patiño, A. Perez-Jiménez, À. Blanco, S. Sánchez, *Adv. Funct. Mater.* **2018**, *28*, 1705086.
[46] a) X. Wang, X.-Z. Chen, C. C. J. Alcântara, S. Sevim, M. Hoop, A. Terzopoulou, C. De Marco, C. Hu, A. J. De Mello, P. Falcaro, S. Furukawa, B. J. Nelson, J. Puigmart-Luis, S. Pané, *Adv. Mater.* **2019**, *31*, 1901592; b) V. Garcia-Gradilla, J. Orozco, S. Sattayasamitsathit, F. Soto, F. Kuralay, A. Pourazary, A. Katzenberg, W. Gao, Y. Shen, J. Wang, *ACS Nano* **2013**, *7*, 9232.
[47] Q.-L. Wang, C. Wang, R.-F. Dong, Q.-Q. Pang, Y.-P. Cai, *Inorg. Chem. Commun.* **2018**, *91*, 1.
[48] A. Szkudlarek, K. E. Hnida-Gut, K. Kollbek, M. M. Marzec, K. Pitala, M. Sikora, *Nanotechnology* **2020**, *31*, 07LT01.
[49] a) M. Nair, R. Guduru, P. Liang, J. Hong, V. Sagar, S. Khizroev, *Nat. Commun.* **2013**, *4*, 1707; b) I. S. M. Khalil, K. Youakim, A. Sanchez, S. Misra, presented at 2014 IEEE/RSJ Int. Conf. *on Intelligent Robots and System*, Chicago, IL, USA, September, **2014**.
[50] P. S. Schattling, M. A. Ramos-Docampo, V. Salgueiriño, B. Städler, *ACS Nano* **2017**, *11*, 3973.
[51] M. Testa-Anta, S. Liébana-Viñas, B. Rivas-Murias, B. Rodríguez González, M. Farle, V. Salgueiriño, *Nanoscale* **2018**, *10*, 20462.
[52] a) T. Li, J. Li, H. Zhang, X. Chang, W. Song, Y. Hu, G. Shao, E. Sandraz, G. Zhang, L. Li, J. Wang, *Small* **2016**, *12*, 6098; b) B. Jang, E. Gutman, N. Stucki, B. F. Seitz, P. D. Wendel-García, T. Newton, J. Pokki, O. Ergeneman, S. Pané, Y. Or, B. J. Nelson, *Nano Lett.* **2015**, *15*, 4829; c) R. Dreyfus, J. Baudry, M. L. Roper, M. Fermigier, H. A. Stone, J. Bibette, *Nature* **2005**, *437*, 862; d) P. Liao, L. Xing, S. Zhang, D. Sun, *Small* **2019**, *15*, 1901197.
[53] a) J. Guo, Z. Liang, Y. Huang, K. Kim, P. Vandeventer, D. Fan, *ACS Nano* **2020**, *14*, 15204; b) Y. Wang, Y. Liu, Y. Li, D. Xu, X. Pan, Y. Chen, D. Zhou, B. Wang, H. Feng, X. Ma, *Research* **2020**, *2020*, 7962024; c) X. Liu, R. Dong, Y. Chen, Q. Zhang, S. Yu, Z. Zhang, X. Hong, T. Li, M. Gao, Y. Cai, *Mater. Today Nano* **2022**, *18*, 100182.
[54] T. Li, A. Zhang, G. Shao, M. Wei, B. Guo, G. Zhang, L. Li, W. Wang, *Adv. Funct. Mater.* **2018**, *28*, 1706066.
[55] G. Yan, B. Xu, X. Shi, Y. Zong, Y. Wu, J. Liu, Y Ouyang, G. Chen, J. Cui, Y. Mei, *Appl. Mater. Today* **2022**, *27*, 101457.
[56] Z. Lin, X. Fan, M. Sun, C. Gao, Q. He, H. Xie, *ACS Nano* **2018**, *12*, 2539.
[57] a) U. Bozuyuk, Y. Alapan, A. Aghakhani, M. Yunusa, M. Sitti, *Proc. Natl. Acad. Sci. USA* **2021**, *118*, e2022090118; b) Y. Alapan, U. Bozuyuk, P. Erkoc, A. C. Karacakol, M. Sitti, *Sci. Rob.* **2020**, *5*, eaba5726.
[58] W. Gao, S. Sattayasamitsathit, K. M. Manesh, D. Weihs, J. Wang, *J. Am. Chem. Soc.* **2010**, *132*, 14403.
[59] H. Morgan, N. G. Green, *AC electrokinetics:colloids and nanoparticles*, Vol. 2, Research Studies Press, **2003**.
[60] H. Li, D. Teal, Z. Liang, H. Kwon, D. Huo, A. Jin, P. Fischer, D. E. Fan, *Nat. Nanotechnol.* **2023**, *18*, 1213.
[61] M. Pal, N. Somalwar, A. Singh, R. Bhat, S. M. Eswarappa, D. K. Saini, A. Ghosh, *Adv. Mater.* **2018**, *30*, 1800429.
[62] a) Y. Ji, X. Lin, Z. Wu, Y. Wu, W. Gao, Q. He, *Angew. Chem., Int. Ed.* **2019**, *58*, 12200; b) T. Cui, Si Wu, Y. Sun, J. Ren, X. Qu, *Nano Lett.* **2020**, *20*, 7350; c) Y. Pan, R. Liu, L. Luo, Z. Song, J. Pan, H. Li, *ACS Sustainable Chem. Eng.* **2023**, *11*, 14723.
[63] J. Wang, *Faraday Discuss.* **2013**, *164*, 9.
[64] S. Il Cho, S. B. Lee, *Acc. Chem. Res.* **2008**, *41*, 699.
[65] J. Li, T. Li, T. Xu, M. Kiristi, W. Liu, Z. Wu, J. Wang, *Nano Lett.* **2015**, *15*, 4814.
[66] A. Serrà, J. García-Torres, *Appl. Mater. Today* **2021**, *22*, 100939.
[67] Y. Mei, A. A. Solovev, S. Sanchez, O. G. Schmidt, *Chem. Soc. Rev.* **2011**, *40*, 2109.

[68] Y. Yin, T. Qiu, L. Ma, X. Lang, Y. Zhang, G. Huang, Y. Mei, O. G. Schmidt, *J. Phys. Chem. C* **2012**, *116*, 25504.
[69] Di Han, Y. Fang, D. Du, G. Huang, T. Qiu, Y. Mei, *Nanoscale* **2016**, *8*, 9141.
[70] X. Fan, Qi Hao, M. Li, X. Zhang, X. Yang, Y. Mei, T. Qiu, *ACS Appl. Mater. Interfaces* **2020**, *12*, 28783.
[71] J. G. Gibbs, N. A. Fragnito, Y. Zhao, *Appl. Phys. Lett.* **2010**, 97.
[72] a) S. Chen, X. Sun, M. Fu, X. Liu, S. Pang, Y. You, X. Liu, Y. Wang, X. Yan, X. Ma, *Biomaterials* **2022**, *288*, 121744; b) Y. Ye, J. Luan, M. Wang, Y. Chen, D. A. Wilson, F. Peng, Y. Tu, *Chem. Eur. J.* **2019**, *25*, 8663.
[73] M. Sun, W. Chen, X. Fan, C. Tian, L. Sun, H. Xie, *Appl. Mater. Today* **2020**, *20*, 100682.
[74] D. Vilela, A. C. Hortelao, R. Balderas-Xicohténcatl, M. Hirscher, K. Hahn, X. Ma, S. Sánchez, *Nanoscale* **2017**, *9*, 13990.
[75] B. Dong, T. Zhou, H. Zhang, C. Y. Li, *ACS Nano* **2013**, *7*, 5192.
[76] S. Liu, D. Xu, J. Chen, Na Peng, T. Ma, F. Liang, *Nanoscale* **2023**, *15*, 12944.
[77] F. Novotný, J. Plutnar, M. Pumera, *Adv. Funct. Mater.* **2019**, *29*, 1903041.
[78] R. A. Alvarez-Puebla, L. M. Liz-Marzán, *Chem. Soc. Rev.* **2012**, *41*, 43.
[79] a) M. K. Gupta, S. Chang, S. Singamaneni, L. F. Drummy, R. Gunawidjaja, R. R. Naik, V. V. Tsukruk, *Small* **2011**, *7*, 1192; b) M. Fernández-Medina, X. Qian, O. Hovorka, B. Städler, *Nanoscale* **2019**, *11*, 733.
[80] a) C. Jiang, Y. Qian, Q. Gao, J. Dong, W. Qian, *J. Mater. Chem.* **2010**, *20*, 8711; b) V. Magdanz, G. Stoychev, L. Ionov, S. Sanchez, O. G. Schmidt, *Angew. Chem.* **2014**, *126*, 2711.
[81] a) E. Caballero-Díaz, C. Pfeiffer, L. Kastl, P. Rivera-Gil, B. Simonet, M. Valcárcel, J. Jiménez-Lamana, F. Laborda, W. J. Parak, *Part. Part. Syst. Charact.* **2013**, *30*, 1079; b) X. Ma, R. Hartmann, D. Jimenez De Aberasturi, F. Yang, S. J. H. Soenen, B. B. Manshian, J. Franz, D. Valdeperez, B. Pelaz, N. Feliu, N. Hampp, C. Riethmüller, H. Vieker, N. Frese, A. Gölzhäuser, M. Simonich, R. L. Tanguay, X.-J. Liang, W. J. Parak, *ACS Nano* **2017**, *11*, 7807.
[82] a) X. Xu, K. Kim, H. Li, D. L. Fan, *Adv. Mater.* **2012**, *24*, 5457; b) J. Liu, J. Guo, G. Meng, D. Fan, *Chem. Mater.* **2018**, *30*, 5256.
[83] X. Xu, H. Li, D. Hasan, R. S. Ruoff, A. X. Wang, D. L. Fan, *Adv. Funct. Mater.* **2013**, *23*, 4332.
[84] C. Gao, Ye Feng, D. A. Wilson, Y. Tu, F. Peng, *Small* **2022**, *18*, 2106263.
[85] W. Duan, R. Liu, A. Sen, *J. Am. Chem. Soc.* **2013**, *135*, 1280.
[86] T. Xu, Y. Luo, C. Liu, X. Zhang, S. Wang, *Anal. Chem.* **2020**, *92*, 7816.
[87] H. Xie, M. Sun, X. Fan, Z. Lin, W. Chen, L. Wang, L. Dong, Q. He, *Sci. Rob.* **2019**, *4*, eaav8006.
[88] K. Zhang, Y. Wang, M. Wu, Y. Liu, D. Shi, B. Liu, *Chem. Sci.* **2018**, *9*, 8089.
[89] L. Guerrini, I. Rodriguez-Loureiro, M. A. Correa-Duarte, Y. H. Lee, X. Y. Ling, F. J García De Abajo, R. A. Alvarez-Puebla, *Nanoscale* **2014**, *6*, 8368.
[90] a) A. K. M. R. H. Chowdhury, B. Tan, K. Venkatakrishnan, *ACS Appl. Mater. Interfaces* **2018**, *10*, 35715; b) K. M. Ostrowska, A. Malkin, A. Meade, J. O'leary, C. Martin, C. Spillane, H. J. Byrne, F. M. Lyng, *Analyst* **2010**, *135*, 3087.
[91] G. Qi, H. Li, Y. Zhang, C. Li, S. Xu, M. Wang, Y. Jin, *Anal. Chem.* **2019**, *91*, 1408.
[92] Y. Chen, R. Pan, Y. Wang, P. Guo, X. Liu, F. Ji, J. Hu, X. Yan, G. P. Wang, Li Zhang, Y. Sun, X. Ma, *Adv. Funct. Mater.* **2022**, *32*, 2200600.
[93] X. Xu, K. Kim, D. Fan, *Angew Chem Int Ed Engl* **2015**, *54*, 2525.
[94] J. Wu, S. Balasubramanian, D. Kagan, K. M. Manesh, S. Campuzano, J. Wang, *Nat. Commun.* **2010**, *1*, 36.
[95] J. Orozco, V. García-Gradilla, M. D'agostino, W. Gao, A. Cortés, J. Wang, *ACS Nano* **2013**, *7*, 818.
[96] C. Liang, C. Zhan, F. Zeng, D. Xu, Y. Wang, W. Zhao, J. Zhang, J. Guo, H. Feng, X. Ma, *ACS Appl. Mater. Interfaces* **2018**, *10*, 35099.
[97] R. A. Álvarez-Puebla, L. M. Liz-Marzán, *Energy Environ. Sci.* **2010**, *3*, 1011.
[98] E. Pazos, M. Garcia-Algar, C. Penas, M. Nazarenus, A. Torruella, N. Pazos-Perez, L. Guerrini, M. E Vázquez, E. Garcia-Rico, J. L. Mascareñas, R. A. Alvarez-Puebla, *J. Am. Chem. Soc.* **2016**, *138*, 14206.
[99] M. Spuch-Calvar, L. Rodríguez-Lorenzo, M. P Morales, R. A. Álvarez-Puebla, L. M. Liz-Marzán, *J. Phys. Chem. C* **2009**, *113*, 3373.
[100] H. Fenniri, R. Alvarez-Puebla, *Nat. Chem. Biol.* **2007**, *3*, 247.
[101] K. Dardir, H. Wang, B. E. Martin, M. Atzampou, C. B. Brooke, L. Fabris, *J. Phys. Chem. C* **2020**, *124*, 3211.
[102] C. Catala, B. Mir-Simon, X. Feng, C. Cardozo, N. Pazos-Perez, E. Pazos, S. Gómez-De Pedro, L. Guerrini, A. Soriano, J. Vila, F. Marco, E. Garcia-Rico, R. A. Alvarez-Puebla, *Adv. Mater. Technol.* **2016**, *1*, 1600163.
[103] D. Jimenez De Aberasturi, A. B. Serrano-Montes, J. Langer, M. Henriksen-Lacey, W. J. Parak, L. M. Liz-Marzán, *Chem. Mater.* **2016**, *28*, 6779.
[104] B. R. Lutz, C. E. Dentinger, L. N. Nguyen, L. Sun, J. Zhang, A. N. Allen, S. Chan, B. S. Knudsen, *ACS Nano* **2008**, *2*, 2306.
[105] M. Liebel, I. Calderon, N. Pazos-Perez, N. F. Van Hulst, R. A. Alvarez-Puebla, *Angew. Chem., Int. Ed.* **2022**, *61*, e202200072.
[106] a) J. Song, J. Zhou, H. Duan, *J. Am. Chem. Soc.* **2012**, *134*, 13458; b) P. Rivera_Gil, C. Vazquez-Vazquez, V. Giannini, M. P Callao, W. J. Parak, M. A. Correa-Duarte, R. A. Alvarez-Puebla, *Angew. Chem., Int. Ed.* **2013**, *52*, 13694.
[107] N. Feliu, X. Sun, R. A. Alvarez Puebla, W. J. Parak, *Langmuir* **2017**, *33*, 6639.
[108] M. Liebel, N. Pazos-Perez, N. F. Van Hulst, R. A. Alvarez-Puebla, *Nat. Nanotechnol.* **2020**, *15*, 1005.
[109] R. Dong, Y. Cai, Y. Yang, W. Gao, B. Ren, *Acc. Chem. Res.* **2018**, *51*, 1940.

I. Brian Becerril-Castro received his B.S. degree in Nanotechnology from the Universidad Nacional Autónoma de México (México) in 2017. He is currently a PhD student under the supervision of Professor Ramon Alvarez-Puebla and Professor Vincenzo Giannini at the Universitat Rovira i Virgili (Spain).

Verónica Salgueiriño received her Ph.D. degree in Chemistry from Universidade de Vigo (Spain) in 2003. She worked as a postdoctoral researcher at the Universität Duisburg-Essen (Germany), Arizona State University (USA), and Universidade de Santiago de Compostela (Spain) until joining Universidade de Vigo in 2009. She currently holds a full professor position and her current research focuses on the magnetic properties of hybrid nanostructures for bio-related applications.

Miguel A. Correa-Duarte earned his Chemistry Ph.D. from the University of Vigo in 2002, followed by postdoctoral roles at CAESAR (Bonn) and as a Visiting Assistant Professor at Arizona State University. Currently a full professor at the University of Vigo's Department of Physical Chemistry, he also directs CINBIO (Research Center of Nanomaterials and Biomedicine). His research focuses on plasmonic photocatalysis, carbon nanotube functionalization, core-shell nanoparticles, and composites.

Ramon A. Alvarez-Puebla is an ICREA Professor at the Universitat Rovira i Virgili in Tarragona. He holds a B.Sc. in Chemistry (Universidad de Navarra, 2000) and a Ph.D. in Surface Science (Universidad Publica de Navarara, 2003). He was a postdoc at the University of Windsor (Windsor, ON, Canada) and General Motors Corporation (Warren, MI, USA) and worked as a Research Officer at the National Institute for Nanotechnology of the National Research Council of Canada (Edmonton, AB, Canada) and as Associate Professor at the Universidade de Vigo.